Study of the performance of fault-tolerant multi-level inverter included in shunt active power filter

Omar Fethi Benaouda[1], Mohamed Mezaache[1], Hind Djeghloud[2], Azzedine Bendiabdellah[3]
[1]Research Center in Industrial Technologies (CRTI), Cheraga, Algeria
[2]Research Laboratory of Electrotechnics, University of Constantine 1, Constantine, Algeria
[3]Diagnostic Group, LDEE Laboratory, Electrical Engineering Faculty, University of Sciences and Technology of Oran Mohamed Boudiaf, El-M'naouer Oran, Algeria

Article Info

ABSTRACT

Nowadays, the large number of shunt active power filters (SAPF) is installed in many grid networks to eliminate the source currents harmonics and enhance power quality. These filters are installed in different places according to the filtration requirements. The connection between SAPF and grid network has a negative effect during the open-circuit fault of the insulated gate bipolar transistor (IGBT) switch of the SAPF. This paper proposes the application of the new diagnostic method based on the trigonometric circle and mean value variations techniques to the early detection and precise location of the open-circuit fault of the IGBT switches, and the inclusion of the modified reconfigurable inverter topology to allow the perfect continuity of the filter currents, and improve the diagnostic of the open-circuit fault. A single-sided amplitude spectrum technique (SSAS) is applied on the source currents to get the THDi% value. The obtained simulation results prove, the great success of the proposed diagnostic method, the ability of the modified reconfigurable inverter to be adapted to the grid network, the short response time between the diagnosis and the reconfiguration process is about 7 ms which is very sufficient to guarantee the rapid continuity of the shunt active power filter.

Corresponding Author:

Omar Fethi Benaouda
Research Center in Industrial Technologies (CRTI)
P.O. Box 64, Cheraga 16014 Algiers, Algeria
Email: benaouda.omar@gmail.com, o.benaouda@crti.dz

1. INTRODUCTION

In the recent years, the growing numbers of non-linear loads in the distribution of grid networks has increased the risks of harmonic pollution. These risks have a negative effect on the energy quality and threaten the stability of the grid networks continuity [1], [2]. To remedy these problems, the passive power filters were firstly installed, to compensate the reactive power, improve the power factor, and reduce the line current harmonic. However, problems of their bulkiness and system resonance are their main disadvantages.

In order to avoid these limitations, the shunt active power filters (SAPF) are found to be an effective solution, to compensate the energy quality, reduce current harmonics and minimize power losses during its transmission from a source to the non-linear load [3], [4]. To achieve these advantages, some scientists are interested to the application of the SAPF in different situations in the grid network, Ouchen *et al.* [5] applied the predictive direct power control for the SAPF, in another study, they incorporated the fuzzy logic technique in the SAPF associated with photovoltaic system to improve the results of the predictive direct power control [6], Dash *et al.* [7] included the harmonic mitigation for the SAPF to reduce the current

harmonics, Sharma *et al.* [8] improved the performance of the SAPF by applying the fractional proportional integral controller. There are other studies that have contributed to the application of the filter techniques that help to reduce the harmonics, among these Saleh *et al.* [9] conducted a comparative study between the nearest level control and the selective harmonic elimination for multi-level inverters, Alhamrouni *et al.* [10] focused on the designing of a topology that contributes in compensating both the reactive power and harmonic currents. Therefore, the SAPF is considered as an ideal resistant to the non-linear load [11].

The SAPFs contain an inverter i.e. a switched system [12] of the power electronic to provide harmonic currents equal to the load currents. There are many topologies of the SAPF that have been presented in literature; Hoon *et al.* [13] suggested a topology of neutral point clamped (NPC) three-level inverter by applying the deviation control, Venkataramanaiah *et al.* [14] suggested several topologies, which may contribute well in improving the performance of the SAPF. The multi-level inverter devices with various topologies are considered as very important tools for energy conversion (DC/AC) that is used to control the drive motors [15]–[19] as well as in compensation of the filter system SAPF of the grid networks. The topology of the used multi-level inverter of the SAPF is considered as a very important solution to increase the produced energy while improving its quality [20]–[22], because it allows in increasing the number of phases [23] and/or its switches, and has big possibility of applying the several different control methods such as (pulse width modulation (PWM) and space vector pulse width modulation (SVPWM)) on its switches [24]–[28]. The large number of semiconductors (IGBTs) is required for the realization of this type of multi-level inverter, however, the several possibilities of faults that may happen in the semiconductors can reduce its reliability [29]–[31]. The majority of faults that occur in the multi-level inverter are either in its switches or its control, for this it can be said that the reliability of power electronics becomes a serious problem [32], [33]. The faults that can occur in the physical semiconductor component of the IGBTs are themselves critical faults [34]. The faults are mainly related to an open or short circuit or to the control of the inverter itself. A lot of researchers have been interested in studying the behavior of the inverter while the fault occurs, as well as the applications of different fault-tolerant topologies to overcome those faults or to mitigate their seriousness; Chen *et al.* [35] include the several strategies of the fault-tolerant control in the T-type three-level inverters under the oscillations of the neutral-point voltage, they have found that the topology could overcome the faults in short time, Duran *et al.* [36] suggested the optimal fault-tolerant control of the parallel inverters to improve the reconfiguration time of the fault-tolerant inverter.

The faults diagnosis (detection, location) is the most important tool especially in the faulty multi-level inverter. There are several techniques for the detection and location of the faulty switches, they are often relied on the currents average values of the Park vector d-q for the fault detection, and examined by the distinguished mean value variations for the fault location [37], [38]. After finishing the diagnosis process, a great attention must be focused on the process of continuity by introducing the concept of redundancy in inverter topologies [39], where the fault-tolerance means keeping the operation with an acceptable performance during the fault occurrence, thanks to the structure and/or control of the reconfigurable inverter [40], [41]. In general, some power devices such as relay switch, fuses, must be added to the fault-tolerant topologies, these devices help to reconfigure the inverter [42]–[44].

This paper proposes a new diagnosis method for the faulty switch of the SAPF inverter, this method based on two techniques; the mean value variations for the early detection and the trigonometric circle for the precise location, the proposed method is applied on a reconfigurable three-level inverter, and in order to know the effect of the open-circuit fault on the source currents, a harmonic spectrum technique of the single-sided amplitude spectrum (SSAS) is suggested to be applied on the source currents to get the THDi% values.

2. MODELING OF SHUNT ACTIVE POWER FILTER (SAPF)

The SAPF is a generator that compensates the non-linear loading current i_L that drains the sinusoidal source current of the grid network in phase with the voltage [9]. Figure 1 shows a schematic diagram of the SAPF. The reference current i_F of the SAPF is generated to guarantee the form of the grid network sinusoidal current i_S, for that, it must be compensated for the load current i_L to cancel the harmonic contents of the current i_S. The SAPF must inject compensated harmonic currents equal but opposite to i_F. So, adding the loading current i_L to the opposite filter current i_F gives the source current i_S.

$$i_S = i_L - i_F \tag{1}$$

$$\begin{bmatrix} V_{s\alpha} \\ V_{s\beta} \end{bmatrix} = \sqrt{\frac{2}{3}} \begin{bmatrix} 1 & -\frac{1}{2} & -\frac{1}{2} \\ 0 & \frac{\sqrt{3}}{2} & -\frac{\sqrt{3}}{2} \end{bmatrix} \begin{bmatrix} V_{sa} \\ V_{sb} \\ V_{sc} \end{bmatrix} \tag{2}$$

The load currents can be given as (3).

$$\begin{bmatrix} i_{s\alpha} \\ i_{s\beta} \end{bmatrix} = \sqrt{\frac{2}{3}} \begin{bmatrix} 1 & -\frac{1}{2} & -\frac{1}{2} \\ 0 & \frac{\sqrt{3}}{2} & -\frac{\sqrt{3}}{2} \end{bmatrix} \begin{bmatrix} i_{sa} \\ i_{sb} \\ i_{sc} \end{bmatrix} \qquad (3)$$

The separation of the homo-polar axis components is considered as an advantage due to the application of the (α-β-0) transformation, where there is no contribution of (α, β) axes in homo-polar components. If the neutral phase is separated from the three-phase system, therefore, no existence of the homo-polar current component that will be eliminated in the simplified (2) and (3) [45], [46]. By using load currents and source voltages, the instantaneous power components p-q are calculated as in (4).

$$\begin{bmatrix} p \\ q \end{bmatrix} = \begin{bmatrix} V_{s\alpha} & V_{s\beta} \\ -V_{s\beta} & V_{s\alpha} \end{bmatrix} \begin{bmatrix} i_{L\alpha} \\ i_{L\beta} \end{bmatrix} \qquad (4)$$

Real and imaginary powers can be divided into two mean components $(\bar{p}, \bar{q})$ and oscillating $(\tilde{p}, \tilde{q})$ as given in (5):

$$\begin{bmatrix} i_{L\alpha} \\ i_{L\beta} \end{bmatrix} = \frac{1}{\Delta} \begin{bmatrix} V_{s\alpha} & -V_{s\beta} \\ V_{s\beta} & V_{s\alpha} \end{bmatrix} \begin{bmatrix} \bar{P} \\ 0 \end{bmatrix} + \frac{1}{\Delta} \begin{bmatrix} V_{s\alpha} & -V_{s\beta} \\ V_{s\beta} & V_{s\alpha} \end{bmatrix} \begin{bmatrix} 0 \\ \bar{q} \end{bmatrix} + \frac{1}{\Delta} \begin{bmatrix} V_{s\alpha} & -V_{s\beta} \\ V_{s\beta} & V_{s\alpha} \end{bmatrix} \begin{bmatrix} \tilde{P} \\ \tilde{q} \end{bmatrix} \qquad (5)$$

The separation between the desired average power components and non-desired $(\bar{p}, \bar{q})$ oscillatory harmonic power components $(\tilde{p}, \tilde{q})$ is inevitable. It helps to calculate the reference currents of the active filter that are injected between source and load. The reference currents of the SAPF are the harmonic components of $i_{L\alpha}$ and $i_{L\beta}$. The grid network voltages, loading currents and the active filter currents are the inputs of the parallel active filter controller, as illustrated in Figure 1.

Figure 1. Schematic diagram of the SAPF

2.1. Open-circuit fault of the inverter IGBTs

To investigate the SAPF operation, an open-circuit fault is induced in the internal switch S^0_{11} of the first leg at t=0.1 s. The spectrum analysis of the source current by applying the SSAS technique helps to

calculate the THDi% value. This section aims to study the effect of a single faulty switch on the performance of the source current.

2.1.1. Results and discussion

Figure 2 shows the spectrum analysis of the source current. Before inducing an open-circuit fault of the switch S^0_{11}, the first leg THDi% value of the source current is equal to 3.06 %, it can be noted that the source currents (i_{sa}, i_{sb}, i_{sc}) have almost sinusoidal forms as shown in Figure 2(a). From 0.1 s and up, they become deformed and imbalanced which lead to the emergence of even and odd harmonics and increased THD value to 10.20% measured in the interval of [0.04 0.2 s], as shown in Figure 2(b). Before inducing the fault, the oscillations of the phase (a) source current i_{sa} are symmetrical with respect to zero. After starting the fault, the i_{sa} oscillates between -60 and 53 A and the different harmonic ranks as reported in Figure 2(a). The fault detection can be noticed easily, however, the faulty switches are localized only by the help of the proposed diagnostic methods that will be seen in the next section.

(a)

(b)
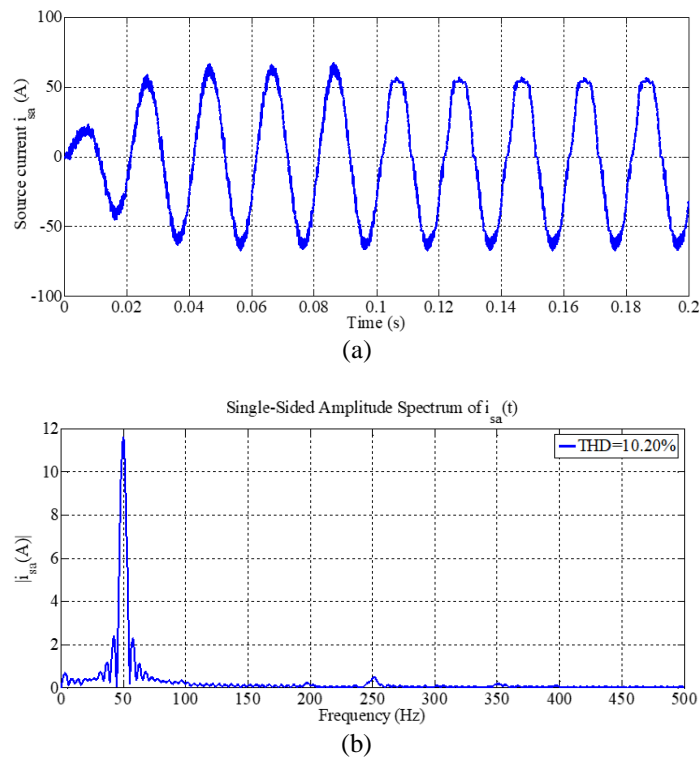
Figure 2. Spectrum analysis of the source current by applying the SSAS technique (a) source current of the first leg i_{sa} and (b) harmonic spectrum of i_{sa} under the open-circuit fault of switch S^0_{11} at 0.1 s

3. METHOD OF DETECTION AND LOCATION OF THE OPEN-CIRCUIT FAULTS
3.1. Fault detection by the mean value of the Park's vector

The Park vectors application is based on the advantage of an average value of currents of the d-q axis during one cycle [47]. The three-phase currents can be transformed into two currents of the d-q axis by the Park transform vector as represented in (8). The average values of currents d-q during one cycle is calculated by (9). The magnitude and angle (argument) are calculated. The two obtained average values can be expressed in a d-q system coordinates by the use of (9).

$$i_d = \frac{2}{3}i_a - \frac{1}{3}(i_b + i_c), i_q = \frac{1}{\sqrt{3}}(i_b - i_c) \tag{6}$$

$$\mu_x = \frac{1}{N}\sum_{K=1}^{N} i_x(k\tau) \tag{7}$$

$$\mu = \mu_d + j\mu_q = M_\mu \angle \theta_\mu \tag{8}$$

$$M_\mu = \sqrt{\mu_d^2 + \mu_q^2}, \theta_\mu = tan^{-1} \frac{\mu_q}{\mu_d} \tag{9}$$

The application of the mean value vector can be applied to the loading and source currents at the same time under the healthy and faulty three-level inverter. An open-circuit fault of the insulated gate bipolar transistor (IGBT) switch can produce disturbances in the source and filter currents. The diagnostic method consists of calculating the average values of the source currents [48]. From these current values, the mean value variations are proposed to detect the faults. The two limits b_1 and b_2 of the mean value variations are put as the instant indicators of the open-circuit fault occurrence. Each fault has its own distinguished trends of the current mean values of the source.

3.1.1. Results and discussion

Before the open-circuit fault occurrence, the mean values of the source currents oscillate within the band limits b_1 and b_2 due to their symmetrical shape. Immediately after the open-circuit fault, the mean values exceed the band limits. At the point where the mean value of the source currents intercepts with one of the band limits is called the instant of the open-circuit detection as well indicated in Figure 3.

3.2. Fault location by application of the trigonometric circle
3.2.1. Results and discussion

The application of the trigonometric circle is used to locate precisely the faulty switch, Figure 4 describes the position of the fault angle θ_μ under the healthy state; the zero-fault angle means that there is not any faulty switch. The trigonometric circle application is designed to locate four faulty switches simultaneously; each one is tested separately as illustrated in Figure 5, an open-circuit fault is induced at 0.1 s, the proposed trigonometric angle trajectories contribute in the extraction of the fault angles of four switches of the first leg which are grouped in Figure 5 and the fault angle interval of each faulty switch is mentioned in Table 1 from the trends of the mean values of the source currents by applying of the mean value variations, and the specific fault angle interval of each faulty switch.
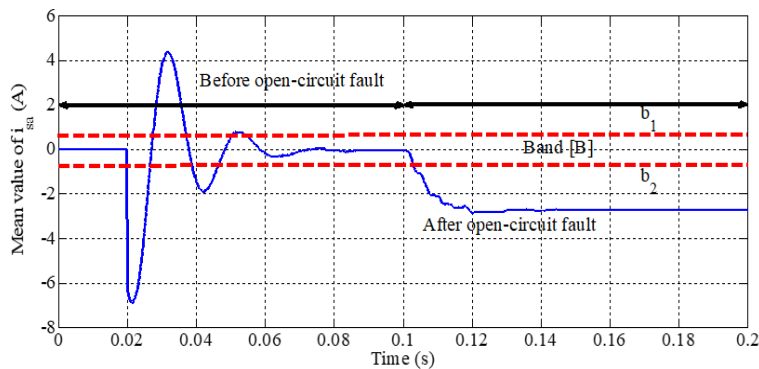

Figure 3. Simulation results of mean value of source current of the first leg under an open-circuit fault of switch S^0_{11}, and examined by the application of the mean value variations
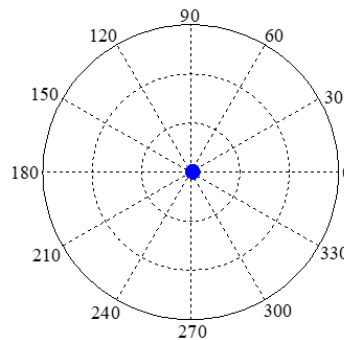

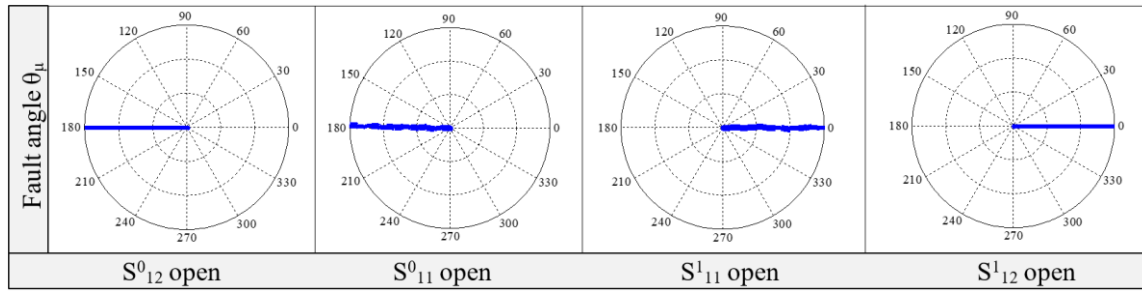Figure 4. Fault angle θ_μ by the trigonometric circle under the healthy state

Figure 5. Graphical representation of the located fault angles by the trigonometric circle application on the source current i_{sa}

Table 1. Location of the open-circuit fault with corresponding to fault angle intervals of the source currents

Open-circuit	Mean value of i_{sa}, i_{sb} and i_{sc}	Interval of θ_μ
S^0_{12} open		$150 < \theta_\mu < 210$
S^0_{11} open		$150 < \theta_\mu < 210$
S^1_{11} open		$330 < \theta_\mu < 30$
S^1_{12} open		$330 < \theta_\mu < 30$
S^0_{22} open		$270 < \theta_\mu < 330$
S^0_{21} open	Exceed the band limits	$270 < \theta_\mu < 330$
S^1_{21} open		$90 < \theta_\mu < 150$
S^1_{22} open		$90 < \theta_\mu < 150$
S^0_{32} open		$30 < \theta_\mu < 90$
S^0_{31} open		$30 < \theta_\mu < 90$
S^1_{31} open		$210 < \theta_\mu < 270$

4. RECONFIGURATION OF THE FAULTY INVERTER

4.1. Topology of the modified reconfigurable inverter

The reconfigurable inverter topology requires the addition of many devices represented in the addition of the active diodes to switches. These devices allow the inverter reconfiguration and obtains new bi-directional current paths [49] as shown in Figure 6. Under an open or short circuit faults, the positive point of the previous topology is the ability to recover the lost voltage. The two types of relays NC (S^0_{U1}, S^1_{U1}, ...) at each leg to isolate any expected open-circuit fault, the relay (S_{NP}) for the neutral point (NP) isolation and the redundant anti-parallel diodes to overcome the faulty freewheel diodes. The relay (S_{NP}) allows for the identification of the two active switches and improves the performance of the faulty inverter. The connection of the relay (S_{NP}) to the neutral point reestablishes the inverter function. When an open-circuit fault occurs at the S^1_{11} switch of phase U_1, the relay (S_{NP}) opens to release the neutral point and allows the exploitation of the alternative configurations. The inverter will operate alternately with the relay switching ($S_{NP'}$) depending on the desired voltage in the faulty leg.
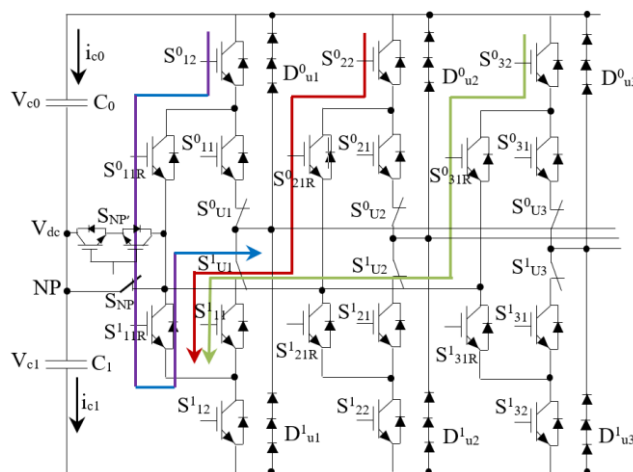

Figure 6. Modified reconfigurable three-level NPC inverter to be integrated into the SAPF

4.1.1. Results and discussion

Figure 7 shows that the THDi% value of the source current of the first leg i_{sa} is equal to 3.96%. It can be concluded that the current of i_{sa} has very little distortion. The proposed diagnostic technique and the modified inverter topology contribute to overcoming the open circuit fault with the concept of fault-tolerant.

Figure 8 illustrates the timeline before and after the fault inclusion. It can be noticed that all detection, location, and reconfiguration processes lasted just 0.007 s. This extremely short time is largely sufficient to guarantee the source current without harmonics which are caused by the open-circuit fault, and also to ensure the continuity of the SAPF.

(a)

(b)
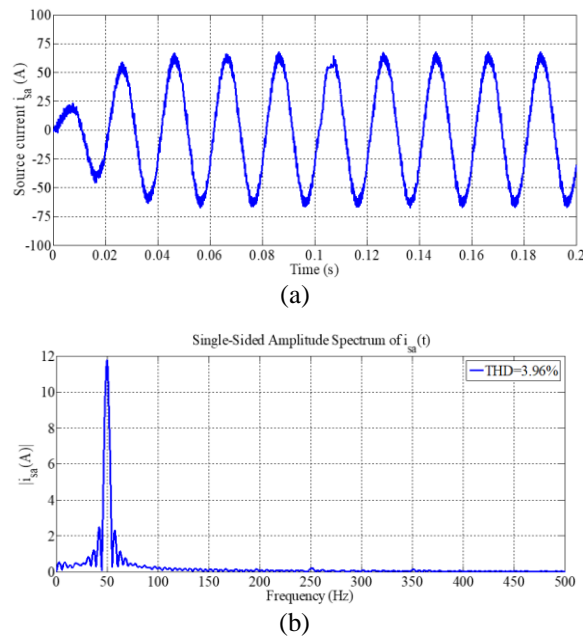
Figure 7. Spectrum analysis of the source current by applying the SSAS technique (a) source current of the first leg i_{sa} and (b) harmonic spectrum of i_{sa} under the open-circuit fault of the SAPF fault-tolerant inverter at switch S^0_{11} at 0.1 s
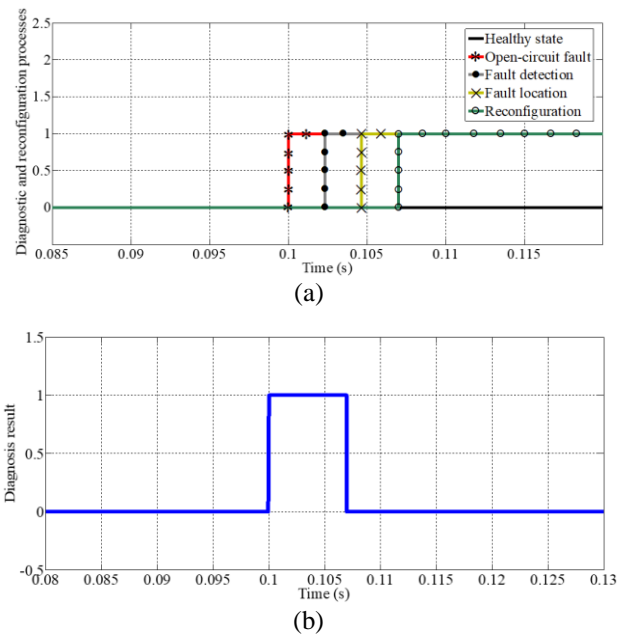
(a)

(b)

Figure 8. Timeline of (a) diagnosis and reconfiguration processes and (b) diagnosis result, under the open-circuit fault at switch S^0_{11} at 0.1 s

Study of the performance of fault-tolerant multi-level inverter included in shunt … (Omar Fethi Benaouda)

5. ROBUSTNESS TESTS OF THE DIAGNOSTIC METHOD UNDER OPEN-CIRCUIT FAULT
5.1. Fault angle value according to the degrading variations

In order to conduct the robustness tests, variables of the input voltage V_{dc} are selected in the Table 2. These variables must be modified by a large variation to know the reliability of the proposed diagnostic method, and to understand the efficiency of the proposed reconfigurable inverter topology during one faulty switch S^0_{11}. Where each variable is modified individually which corresponds to a localized fault angle for each variation.

Table 2. Variations of the input voltage V_{dc}

Variable	Symbol	Value (V)
V_{dc}	V_1	400
	V_2	450
	V_3	500
	V_4	550
	V_5	600

5.1.1. Results and discussion

Figure 9, shows the location of open-circuit fault of the switch S^0_{11} by applying the variations of all the input voltage V_{dc}, as shown in Table 2. From the obtained results of Figure 9, it can be concluded that the fault angle values are not affected by the modification any mentioned variables in the previous table, because the fault angles are limited between 150 and 210, as shown in the Figure 9, this means that the proposed diagnostic method is successful to precise locating under the degraded values of all selected variable, thanks to the trigonometric circle technique, the fault angles can be located even under severe conditions.
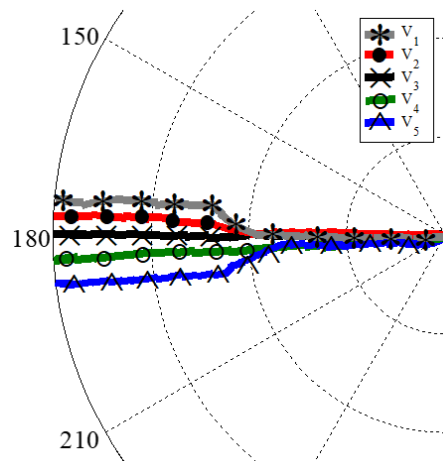

Figure 9. Fault angle locations of the open-circuit at the switch S^0_{11} according to the variation of input voltage V_{dc}

6. CONCLUSION

In this paper, the shunt active parallel filter (SAPF) model with voltage V_{dc} regulator is presented in order to reduce the negative effect of the source current distortion harmonics caused by the non-linear load. The harmonic spectrum technique of the single-sided amplitude spectrum (SSAS) is applied on the source currents to get the THDi% values. In the healthy state, the first leg THDi% values of the source current is equal to 3.06 %. In the faulty state, the open-circuit fault is included in one switch of the three-level inverter of the SAPF, the THDi% value of the source current of the faulty leg is equal to 10.20%, this big increase of the THDi% values allow to propose a diagnostic method that is based on the techniques of the trigonometric circle and mean value variations to detect and locate the open-circuit fault of the IGBT switches, the obtained results prove the efficiency of the proposed diagnostic method in terms of the early detection and precise location of the faulty switch. Moreover, in this paper, the proposed fault-tolerant inverter topology has been included in the SAPF. In order to know the performance of the reconfigurable inverter under an open-circuit fault of the switch, the obtained results of the faulty leg using the THDi% values prove the reconfiguration

performance; where the THDi% values of the source current are equal to 3.96%. In addition, the time for diagnosis and reconfiguration processes is estimated to 0.007s which is extremely short and appropriate to ensure the perfect continuity of the filter process. After confirming that the fault-tolerant inverter is successfully incorporated with the proposed diagnostic method, the robustness tests are applied on the faulty inverter of the SAPF with the degraded parameters of the input voltage V_{dc} of the reconfigurable inverter. The obtained results are very motivating in terms of the early detection and precise location of the open-circuit fault and the fast reconfiguration of the proposed fault-tolerant inverter of the SAPF. For future prospects, it would be better to apply the proposed diagnostic method on other domains that interested in the application of converters. This will be the scope of a future paper.

ACKNOWLEDGEMENTS

REFERENCES

[1]   N. Locci, C. Muscas, and S. Sulis, "Detrimental effects of capacitors in distribution networks in the presence of harmonic pollution," *IEEE Transactions on Power Delivery*, vol. 22, no. 1, pp. 311–315, Jan. 2007, doi: 10.1109/TPWRD.2006.877088.
[2]   S.-H. Jo, S. Son, and J.-W. Park, "On improving distortion power quality index in distributed power grids," *IEEE Transactions on Smart Grid*, vol. 4, no. 1, pp. 586–595, Mar. 2013, doi: 10.1109/TSG.2012.2222943.
[3]   T.-T. Chang and H.-C. Chang, "An efficient approach for reducing harmonic voltage distortion in distribution systems with active power line conditioners," *IEEE Transactions on Power Delivery*, vol. 15, no. 3, pp. 990–995, Jul. 2000, doi: 10.1109/61.871364.
[4]   H. Wang and S. Liu, "Harmonic interaction analysis of delta-connected cascaded h-bridge-based shunt active power filter," *IEEE Journal of Emerging and Selected Topics in Power Electronics*, vol. 8, no. 3, pp. 2445–2460, Sep. 2020, doi: 10.1109/JESTPE.2019.2930033.
[5]   S. Ouchen, A. Betka, J.-P. Gaubert, and S. Abdeddaim, "Simulation and real time implementation of predictive direct power control for three phase shunt active power filter using robust phase-locked loop," *Simulation Modelling Practice and Theory*, vol. 78, pp. 1–17, Nov. 2017, doi: 10.1016/j.simpat.2017.08.003.
[6]   S. Ouchen, A. Betka, S. Abdeddaim, and A. Menadi, "Fuzzy-predictive direct power control implementation of a grid connected photovoltaic system, associated with an active power filter," *Energy Conversion and Management*, vol. 122, pp. 515–525, Aug. 2016, doi: 10.1016/j.enconman.2016.06.018.
[7]   R. Dash, P. Paikray, and S. C. Swain, "Active power filter for harmonic mitigation in a distributed power generation system," in *2017 Innovations in Power and Advanced Computing Technologies (i-PACT)*, Apr. 2017, pp. 1–6, doi: 10.1109/IPACT.2017.8245204.
[8]   R. Sharma, N. Goel, and S. Chacko, "Performance investigation of fractional PI controller in shunt active filter for a three phase four wire system," in *2018 4th International Conference on Computing Communication and Automation (ICCCA)*, Dec. 2018, pp. 1–7, doi: 10.1109/CCAA.2018.8777576.
[9]   W. A. A. Saleh, N. A. M. Said, W. A. Halim, and A. Jidin, "Comparison between selective harmonic elimination and nearest level control for transistor clamped H-bridge inverter," *Indonesian Journal of Electrical Engineering and Computer Science (IJEECS)*, vol. 26, no. 1, pp. 46–55, Apr. 2022, doi: 10.11591/ijeecs.v26.i1.pp46-55.
[10] I. Alhamrouni, F. N. Hanafi, M. Salem, N. H. A. Rahman, A. Jusoh, and T. Sutikno, "Design of shunt hybrid active power filter for compensating harmonic currents and reactive power," *Telecommunication Computing Electronics and Control (TELKOMNIKA)*, vol. 18, no. 4, Aug. 2020, doi: 10.12928/telkomnika.v18i4.15156.
[11] M. Lamich, J. Balcells, M. Corbalan, and E. Griful, "Nonlinear loads model for harmonics flow prediction, using multivariate regression," *IEEE Transactions on Industrial Electronics*, vol. 64, no. 6, pp. 4820–4827, Jun. 2017, doi: 10.1109/TIE.2017.2674596.
[12] D. P. Nam, N. H. Quang, N. N. Tung, and T. T. H. Yen, "Adaptive dynamic programming algorithm for uncertain nonlinear switched systems," *International Journal of Power Electronics and Drive Systems (IJPEDS)*, vol. 12, no. 1, pp. 551–557, Mar. 2021, doi: 10.11591/ijpeds.v12.i1.pp551-557.
[13] Y. Hoon, M. A. M. Radzi, M. K. Hassan, and N. F. Mailah, "Neutral-point voltage deviation control for three-level inverter-based shunt active power filter with fuzzy-based dwell time allocation," *IET Power Electronics*, vol. 10, no. 4, pp. 429–441, Mar. 2017, doi: 10.1049/iet-pel.2016.0240.
[14] J. Venkataramanaiah, Y. Suresh, and A. K. Panda, "A review on symmetric, asymmetric, hybrid and single DC sources based multilevel inverter topologies," *Renewable and Sustainable Energy Reviews*, vol. 76, pp. 788–812, Sep. 2017, doi: 10.1016/j.rser.2017.03.066.
[15] A. B. Salih, Z. S. Mahmood, A. H. M. Ali, and A. N. Nasret, "Enhancement of motor speed identification using artificial neural networks," *Indonesian Journal of Electrical Engineering and Computer Science (IJEECS)*, vol. 27, no. 3, pp. 1388–1396, Sep. 2022, doi: 10.11591/ijeecs.v27.i3.pp1388-1396.
[16] S. K. K. Sampathkumar and D. P. Kumar, "Power quality assessment of novel multilevel and multistring inverters for electric vehicle applications," *Bulletin of Electrical Engineering and Informatics*, vol. 11, no. 4, pp. 1818–1827, Aug. 2022, doi: 10.11591/eei.v11i4.3512.
[17] Y. S. Babu and K. C. Sekhar, "Five-phase induction motor drive for electric vehicle with high gain switched-inductor quasi impedance source inverter," *International Journal of Power Electronics and Drive Systems (IJPEDS)*, vol. 13, no. 1, pp. 411–422, Mar. 2022, doi: 10.11591/ijpeds.v13.i1.pp411-422.
[18] A. H. Shallal, A. F. Nashee, and A. E. Abbas, "Smart actuator for IM speed control with F28335 DSP application," *Indonesian Journal of Electrical Engineering and Computer Science (IJEECS)*, vol. 24, no. 3, pp. 1421–1431, Dec. 2021, doi: 10.11591/ijeecs.v24.i3.pp1421-1431.
[19] C. D. Tran, T. X. Nguyen, and P. D. Nguyen, "A field-oriented control (FOC) method using the virtual currents for the induction motor drive," *International Journal of Power Electronics and Drive Systems (IJPEDS)*, vol. 12, no. 4, pp. 2095–2102, Dec. 2021, doi: 10.11591/ijpeds.v12.i4.pp2095-2102.

[20] S. Raj, R. K. Mandal, M. De, and A. K. Singh, "Nine-level inverter with lesser number of power semiconductor switches using dSPACE," *International Journal of Power Electronics and Drive Systems (IJPEDS)*, vol. 13, no. 1, pp. 39–46, Mar. 2022, doi: 10.11591/ijpeds.v13.i1.pp39-46.

[21] H. Javvaji and B. Banakara, "An enhanced 17-level hybridized multilevel inverter with stair case modulation," *International Journal of Power Electronics and Drive Systems (IJPEDS)*, vol. 11, no. 4, pp. 1872–1882, Dec. 2020, doi: 10.11591/ijpeds.v11.i4.pp1872-1882.

[22] M. Setti and M. Cherkaoui, "Design and implementation of an optimized multilevel power inverter structure based on C MEX and PSPICE," *International Journal of Power Electronics and Drive Systems (IJPEDS)*, vol. 11, no. 3, pp. 1388–1397, Sep. 2020, doi: 10.11591/ijpeds.v11.i3.pp1388-1397.

[23] M. Nekkaz, A. Djahbar, and R. Taleb, "Modeling and control of two five-phase induction machines connected in series powered by matrix converter," *International Journal of Power Electronics and Drive Systems (IJPEDS)*, vol. 12, no. 2, pp. 685–694, Jun. 2021, doi: 10.11591/ijpeds.v12.i2.pp685-694.

[24] O. A. Elkholi, M. A. Enany, A. F. Abdo, and M. Eid, "Novel approach for SVPWM of two-level inverter fed induction motor drive," *International Journal of Power Electronics and Drive Systems (IJPEDS)*, vol. 11, no. 4, pp. 1750–1758, Dec. 2020, doi: 10.11591/ijpeds.v11.i4.pp1750-1758.

[25] M. Van Chung, D. T. Anh, P. Vu, and L. M. Nguyen, "Hardware in the loop co-simulation of finite set-model predictive control using FPGA for a three level CHB inverter," *International Journal of Power Electronics and Drive Systems (IJPEDS)*, vol. 11, no. 4, pp. 1719–1730, Dec. 2020, doi: 10.11591/ijpeds.v11.i4.pp1719-1730.

[26] D. Karthikeyan, K. Vijayakumar, D. Senthil Kumar, and D. Krishnachaitanya, "Mathematical analysis of cost function and reliability condition for new proposed multilevel inverter topology," *Indonesian Journal of Electrical Engineering and Computer Science (IJEECS)*, vol. 20, no. 2, pp. 654–661, Nov. 2020, doi: 10.11591/ijeecs.v20.i2.pp654-661.

[27] C. Laoufi, Z. Sadoune, A. Abbou, and M. Akherraz, "New model of electric traction drive based sliding mode controller in field-oriented control of induction motor fed by multilevel inverter," *International Journal of Power Electronics and Drive Systems (IJPEDS)*, vol. 11, no. 1, pp. 242–250, Mar. 2020, doi: 10.11591/ijpeds.v11.i1.pp242-250.

[28] A. M. Razali, N. A. Yusoff, K. A. Karim, A. Jidin, and T. Sutikno, "A new switching look-up table for direct power control of grid connected 3L-NPC PWM rectifier," *International Journal of Power Electronics and Drive Systems (IJPEDS)*, vol. 12, no. 3, pp. 1413–1421, Sep. 2021, doi: 10.11591/ijpeds.v12.i3.pp1413-1421.

[29] O. F. Benaouda, A. Bendiabdellah, and B. D. E. Cherif, "Contribution to reconfigured multi-level inverter fed double stator induction machine DTC-SVM control," *International Review on Modelling and Simulations (IREMOS)*, vol. 9, no. 5, Oct. 2016, doi: 10.15866/iremos.v9i5.10053.

[30] K. Sodha, G. Fernandez S., V. K., and S. D., "A novel collective health monitoring of a wind park," *Indonesian Journal of Electrical Engineering and Computer Science (IJEECS)*, vol. 21, no. 2, pp. 625–634, Feb. 2021, doi: 10.11591/ijeecs.v21.i2.pp625-634.

[31] M. Azimi and H. T. Shandiz, "An LMI approach to Mixed H_∞/H_- fault detection observer design for linear fractional-order systems," *Telecommunication Computing Electronics and Control (TELKOMNIKA)*, vol. 19, no. 6, Dec. 2021, doi: 10.12928/telkomnika.v19i6.18741.

[32] F. Wani *et al.*, "Lifetime analysis of IGBT power modules in passively cooled tidal turbine converters," *Energies*, vol. 13, no. 8, Apr. 2020, doi: 10.3390/en13081875.

[33] S. R. Mestha and A. J. P. Pius, "Investigation of reliability assessement in power electronics circuits using machine learning," *International Journal of Power Electronics and Drive Systems (IJPEDS)*, vol. 12, no. 1, pp. 558–566, Mar. 2021, doi: 10.11591/ijpeds.v12.i1.pp558-566.

[34] M. Manap, S. Nikolovski, A. Skamyin, R. Karim, T. Sutikno, and M. H. Jopri, "An analysis of voltage source inverter switches fault classification using short time Fourier transform," *International Journal of Power Electronics and Drive Systems (IJPEDS)*, vol. 12, no. 4, pp. 2209–2220, Dec. 2021, doi: 10.11591/ijpeds.v12.i4.pp2209-2220.

[35] J. Chen, C. Zhang, A. Chen, and X. Xing, "Fault-tolerant control strategies for T-Type three-level inverters considering neutral-point voltage oscillations," *IEEE Transactions on Industrial Electronics*, vol. 66, no. 4, pp. 2837–2846, Apr. 2019, doi: 10.1109/TIE.2018.2842731.

[36] M. J. Duran, I. G. Prieto, M. Bermudez, F. Barrero, H. Guzman, and M. R. Arahal, "Optimal fault-tolerant control of six-phase induction motor drives with parallel converters," *IEEE Transactions on Industrial Electronics*, vol. 63, no. 1, pp. 629–640, Jan. 2016, doi: 10.1109/TIE.2015.2461516.

[37] B. D. E. Cherif, A. Bendiabdellah, and M. A. Khelif, "Detection of open-circuit fault in a three-phase voltage inverter fed induction motor," *International Review of Automatic Control (IREACO)*, vol. 9, no. 6, Nov. 2016, doi: 10.15866/ireaco.v9i6.10268.

[38] A. Anand, N. Raj, S. George, and Jagadanand G, "Open switch fault detection in Cascaded H-Bridge multilevel inverter using normalised mean voltages," in *2016 IEEE 6th International Conference on Power Systems (ICPS)*, Mar. 2016, pp. 1–6, doi: 10.1109/ICPES.2016.7584128.

[39] S. Zerdani, M. L. Elhafyani, H. Fadil, and S. Zouggar, "Newly fault-tolerant indirect vector control for traction inverter," *International Journal of Power Electronics and Drive Systems (IJPEDS)*, vol. 12, no. 3, pp. 1576–1585, Sep. 2021, doi: 10.11591/ijpeds.v12.i3.pp1576-1585.

[40] H. K. Jahan, F. Panahandeh, M. Abapour, and S. Tohidi, "Reconfigurable multilevel inverter with fault-tolerant ability," *IEEE Transactions on Power Electronics*, vol. 33, no. 9, pp. 7880–7893, Sep. 2018, doi: 10.1109/TPEL.2017.2773611.

[41] M. M. Haji-Esmaeili, M. Naseri, H. Khoun-Jahan, and M. Abapour, "Fault-tolerant structure for cascaded H-bridge multilevel inverter and reliability evaluation," *IET Power Electronics*, vol. 10, no. 1, pp. 59–70, Jan. 2017, doi: 10.1049/iet-pel.2015.1025.

[42] M. Aleenejad and R. Ahmadi, "Fault-tolerant multilevel cascaded H-bridge inverter using impedance-sourced network," *IET Power Electronics*, vol. 9, no. 11, pp. 2186–2195, Dec. 2016, doi: 10.1049/iet-pel.2016.0033.

[43] U.-M. Choi, K.-B. Lee, and F. Blaabjerg, "Diagnosis and tolerant strategy of an open-switch fault for T-Type three-level inverter systems," *IEEE Transactions on Industry Applications*, vol. 50, no. 1, pp. 495–508, Jan. 2014, doi: 10.1109/TIA.2013.2269531.

[44] K. Saleh and O. Mahmoud, "Asymmetrical four-wire cascaded h-bridge multi-level inverter based shunt active power filter supplied by a photovoltaic source," *International Journal of Power Electronics and Drive Systems (IJPEDS)*, vol. 12, no. 3, pp. 1673–1686, Sep. 2021, doi: 10.11591/ijpeds.v12.i3.pp1673-1686.

[45] H. Akagi, Y. Kanazawa, K. Fujita, and A. Nabae, "Generalized theory of instantaneous reactive power and its application," *Electrical Engineering in Japan*, vol. 103, no. 4, pp. 58–66, Jul. 1983, doi: 10.1002/eej.4391030409.

[46] E. Clark, "Circuit analysis of A.C. power systems. Vol. II," *Students Quarterly Journal*, vol. 22, no. 86, 1951, doi: 10.1049/sqj.1951.0080.

[47] H. Guo, S. Guo, J. Xu, and X. Tian, "Power switch open-circuit fault diagnosis of six-phase fault tolerant permanent magnet synchronous motor system under normal and fault-tolerant operation conditions using the average current Park's vector approach," *IEEE Transactions on Power Electronics*, vol. 36, no. 3, pp. 2641–2660, Mar. 2021, doi: 10.1109/TPEL.2020.3017637.

[48] Y. Yang, L. Ke, and Y. Liu, "Fault detection method of modular multilevel converter based on current mean value and SVM," in *2020 Chinese Control and Decision Conference (CCDC)*, Aug. 2020, pp. 4058–4063, doi: 10.1109/CCDC49329.2020.9164798.

[49] J. F. Silva and S. F. Pinto, "Control methods for switching power converters," in *Power Electronics Handbook*, Elsevier, 2007, pp. 935–998.

BIOGRAPHIES OF AUTHORS

Omar Fethi Benaouda ⓘ 🔗 SC ◖ received the B.Tech degree from the University of Djelfa, Algeria, in 2009, and an M.Tech degree in Electrical Engineering from the University of Sciences and Technology of Oran, (USTO-MB) Algeria, in 2013, and the Ph.D. degree from the University of Sciences and Technology of Oran (USTO-MB), Algeria, in 2017. He is currently a senior researcher at the Research Centre in Industrial Technologies-CRTI, Algiers, Algeria and member of the Diagnostic Group, LDEE laboratory at University of Sciences and Technology of Oran since 2010. His areas of interest are control of electrical machines, artificial intelligence (fuzzy logic, neuron network), multi-level converters, and fault-tolerant. He can be contacted at email: benaouda.omar@gmail.com.

Mohamed Mezaache ⓘ 🔗 SC ◖ received his B.Tech degree, from the University of Batna, Algeria, in 2008, and M.Tech degree in Electrical Engineering from University of Batna, Algeria, in 2011, and the Ph.D. degree from the University of Batna, Algeria, in 2016. He is currently a senior researcher at the Research Centre in Industrial Technologies-CRTI, Algiers, Algeria. His research interests include electrical networks, power electronics, artificial intelligence techniques, welding and related techniques. He can be contacted at email: m.mezaache@crti.dz.

Hind Djeghloud ⓘ 🔗 SC ◖ received her B.Tech, M.Tech. and Ph.D. degrees in Electric Machines from the Department of Electrotechnics of Constantine University, Algeria, respectively in 2000, 2002, and 2007. By 2003, she joined the department of Electrotechnics, at Constantine University Algeria, as an Assistant Professor. Now, she is a lecturer in the same department and is interested by power electronics including electric power quality, active power filters, PWM converters, and renewable energy systems. She can be contacted at email: hinddjeghloud@yahoo.fr.

Azzedine Bendiabdellah ⓘ 🔗 SC ◖ Member of IEEE, received his BE degree with honors and his Ph.D. degree from the University of Sheffield, England, in 1980, and 1985 respectively. From 1990 to 1991 he was a visiting professor at Tokyo institute of technology (T.I.T), Japan. He is currently Professor of Electrical Engineering and Head of the Diagnostic Group, LDEE Laboratory at the University of Sciences and Technology of Oran, (USTO-MB) Algeria. His research interests include electrical machines and drives analysis and modelling, electrical machines and drives control, electrical machines and drives diagnosis and fault tolerance. He can be contacted at email: bendiazz@yahoo.fr.